Bifurcation-Based Transient Stability Analysis of Grid-Forming Converters with DC-Link Voltage Controller

2021 IEEE 22nd Workshop on Control and Modelling of Power Electronics (COMPEL) | 978-1-6654-3635-9/21/$31.00 ©2021 IEEE | DOI: 10.1109/COMPEL52922.2021.9646045

[1]Cheng Luo, [2]Teng Liu, [2]Xiongfei Wang, [1]Xikui Ma
1. School of Electrical Engineering, Xi'an Jiaotong University, Xi'an, China
2. Dept. of AAU Energy, Aalborg University, Aalborg, Denmark
cluo@et.aau.dk, teli@energy.aau.dk, xwa@energy.aau.dk, maxikui@xjtu.edu.cn

***Abstract*—Transient stability of grid-forming (GFM) converters has drawn increasing research interests in the last few years, while the impact of DC-Link Voltage Controller (DVC) on the transient stability of GFM converters remains an open issue. To bridge this research gap, this paper presents a design-oriented transient stability analysis of GFM converters with DVC. A large-signal model is established first. Based on this model, the parametric effects of DVC on the transient stability are evaluated by phase portraits and further confirmed by simulation tests. It is revealed that the increase of proportional gain of DVC would enhance the transient stability. The mechanism of the parametric effects is theoretically explained based on the bifurcation theory. Finally, experimental tests are performed to validate the effectiveness of the theoretical analysis.**

Keywords—Transient stability, grid-forming converters, DC-Link voltage controller, bifurcation theory.

I. INTRODUCTION

Grid-connected converters play a vital role in the utilization of renewable energy sources such as photovoltaics and wind power, and are key equipment for reducing carbon emission in the power industry [1]. As one representative type of grid-connected converters, Grid-Forming (GFM) converters have developed vigorously in the past decade due to their superior applicability under weak grid conditions [2].

Compared with the abundant small-signal stability studies of GFM converters, there are only a few researches on the transient stability analysis of GFM converters, i.e., the ability of GFM converters to maintain synchronism with the grid under large disturbances [3]-[4]. The transient stability of GFM converters is analyzed by phase portrait in [5], revealing that the instability of the system with equilibrium point after fault is mainly due to weak damping. The increase of the cut-off frequency for the active power loop filter can enhance the transient stability. In [6], the control scheme of the GFM converter is compared with the control scheme of the synchronous generator. Then the Lyapunov energy function is used to reveal the effect of equivalent damping on improving transient stability. In [7], limit cycle is used to explain the oscillation phenomenon of GFM converter when it loses synchronism with the grid. Most of the existing works consider that the DC-Link voltage of the GFM converter is generally taken over by a front-end converter, which, thus, allows the assumption of a constant DC-Link voltage. Nevertheless, field applications show the fact that the GFM converter can also be equipped with the DVC to keep a constant DC-Link voltage by itself [1], [8]. Up to now, the impact of DVC on the transient stability of GFM converters has not been systematically studied yet. On the other hand, the order of GFM converters will be increased to at least three order when including DVC. The existing analytical methods e.g. equivalent damping method [5] or equal area criterion method [9], cannot be applied into GFM converters to reveal the mechanism behind parametric effects. Therefore, the transient stability of GFM converters including DVC as well as the mechanism behind parametric effects still remain an open issue.

This article attempts to bridge these research gaps. The large-signal model of GFM converter with DVC is derived first. After that, the phase portrait is used to analyze the parametric effects of DVC on the transient stability, where the obtained results are further validated by the simulation tests. Then the internal mechanism behind parametric effects is explained by the bifurcation theory. Finally, the experiments verify the effectiveness of the theoretical analysis.

II. Transient Stability Analysis of GFM converter with DVC

A. System Strcture

TABLE I
MAIN SYSTEM PARAMETERS

Symbol	Item	Value
V_g	Grid voltage (*l-g*, rms)	40V
E_0	Rated voltage	40V
L_g	Grid inductance	8mH
V_{dc}^{ref}	Rated DC-link Voltage	400V
f_{sw}	Switching frequency	10000Hz
C_f	Filter capacitor	20μF
L_f	Filter inductor	3mH
P_d	Rated active power	640W
Q_0	Rated reactive power	0 Var
L_v	Virtual inductance	4mH
C_{dc}	DC-side Capacitor	450μF
f_0	Fundamental frequency	50Hz
k_{pf}	*P-f* droop coefficient	0.0126
k_{idc}	integral gain of the DVC	0.025
k_{pdc}	proportional gain of the DVC	0.004

Fig. 1 shows the single-line diagram of a grid-connected three-phase GFM converters with synchronous power controller [10], where P_d denotes the power injected to the

This work was supported by China Scholarship Council under Grant 202006280458.

978-1-6654-3635-9/21/$31.00 ©2021 IEEE

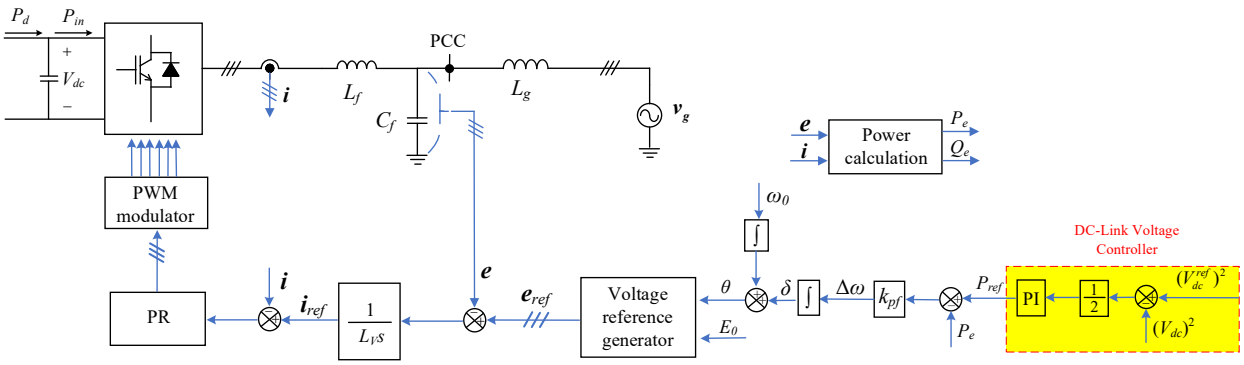

Fig. 1: Single-line diagram of a three-phase SPC-controlled GFM converter with DC-Link voltage controller

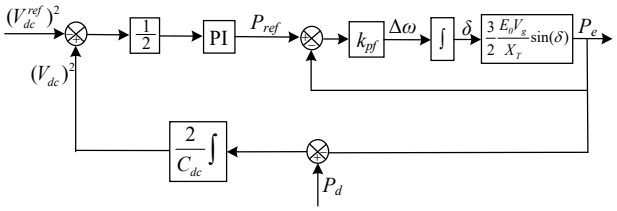

Fig. 2: Simplified large-signal model of GFM converter for transient stability analysis

GFM converters. L_f and C_f constitute the output LC filter. L_g represents the grid inductance. L_v represents the virtual inductance. V_{dc} and $\boldsymbol{v}_g$ denote the DC-Link voltage and grid voltage, respectively. $\boldsymbol{e}$ represents the voltage at the point of common coupling (PCC). $\boldsymbol{i}$ denotes the converter-side current. E and θ represent the magnitude and phase angle of the voltage reference $\boldsymbol{e}_{ref}$, respectively.

The DC-Link voltage of the GFM converters is controlled by PI controller, as highlighted in the yellow box in Fig. 1. This study focuses on analyzing the influence of the PI parameters on the transient stability. Due to the similarity of the influence analysis steps of k_{pdc} and k_{idc}, it only discusses the influence of k_{pdc} in this article. In the following analysis, k_{idc} always remains unchanged.

B. Transient stability analysis based on phase portrait and simulation

The grid fault in this paper is that the grid voltage magnitude drops from 1.0 p.u. to 0.6 p.u., and this voltage fault does not trigger current saturation. The dynamic of the power loop and DVC loop is much slower than that of the inner voltage loop and current loop. Hence, the inner voltage loop and current loop could be omitted when analyzing the transient stability [11]-[12]. The simplified control diagram is show in Fig. 2.

The large-signal model of the system according to the simplified control diagram is derived as differential algebraic equations (1)-(2).

$$\begin{cases} \dot{\delta} = k_{pf}\left(P_{ref} - P_e\right) \\ \dot{(V_{dc}^2)} = \dfrac{2}{C_{dc}}\left(P_d - P_e\right) \\ \Delta\dot{P}_{ref} = \dfrac{1}{2}k_{idc}\left((V_{dc})^2 - \left(V_{dc}^{ref}\right)^2\right) + \dfrac{k_{pdc}}{C_{dc}}\left(P_d - P_e\right) \end{cases} \tag{1}$$

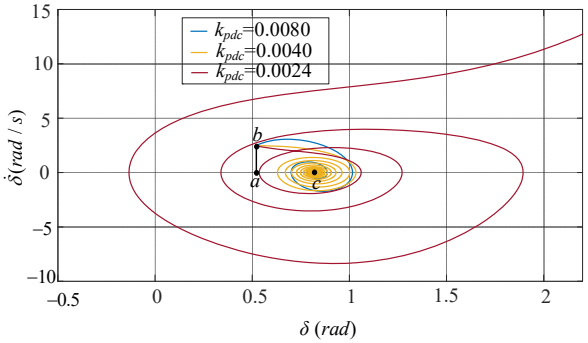

Fig. 3: Phase portraits of the GFM converter with the decrease of k_{pdc}.

$$P_e = \frac{3}{2}\frac{E_0 V_g \sin(\delta)}{X_T} \tag{2}$$

where, $X_T = X_v + X_g$ denotes the total impedance of the system.

The ODE45 function of MATLAB could be used to obtain the phase portrait of the system, which reflects the law of parametric effects [13]. When studying the parametric effects of the DVC on transient stability, the main task is to analyze the influence of the k_{pdc} on phase portraits.

The necessary condition for the transient stability is that the differential equation (1) have equilibrium point after fault, which means that equation (3) need to be satisfied.

$$P_d = P_e \quad V_{dc} = V_{dc}^{ref} \quad P_{ref} = P_d \tag{3}$$

According to equation (3), the equilibrium point is not affected by k_{pdc}. When adopting the main system parameters as shown in Table I, there always exists equilibrium point when the grid voltage magnitude drops form 1.0 p.u. to 0.60 p.u. k_{pdc} only affects whether the system can reach the new equilibrium point. The phase portraits under different k_{pdc} are shown in Fig. 3.

In Fig. 3, point a represents initial operating point of the system, and point c represents the equilibrium point of the system after fault. When grid voltage fault occurs, the operating point of the system always changes from point a to point b, and then gradually converges to point c or diverges to infinity. When keeping k_{idc} unchanged and decreasing k_{pdc}, phase portraits gradually cannot converge to point c. Hence, reducing k_{pdc} will weaken the transient stability of the system. Therefore, when designing DVC parameters, a large k_{pdc} is recommended.

The SIMULINK verification results are shown in Fig. 4, which are the power angles of the GFM converter after fault

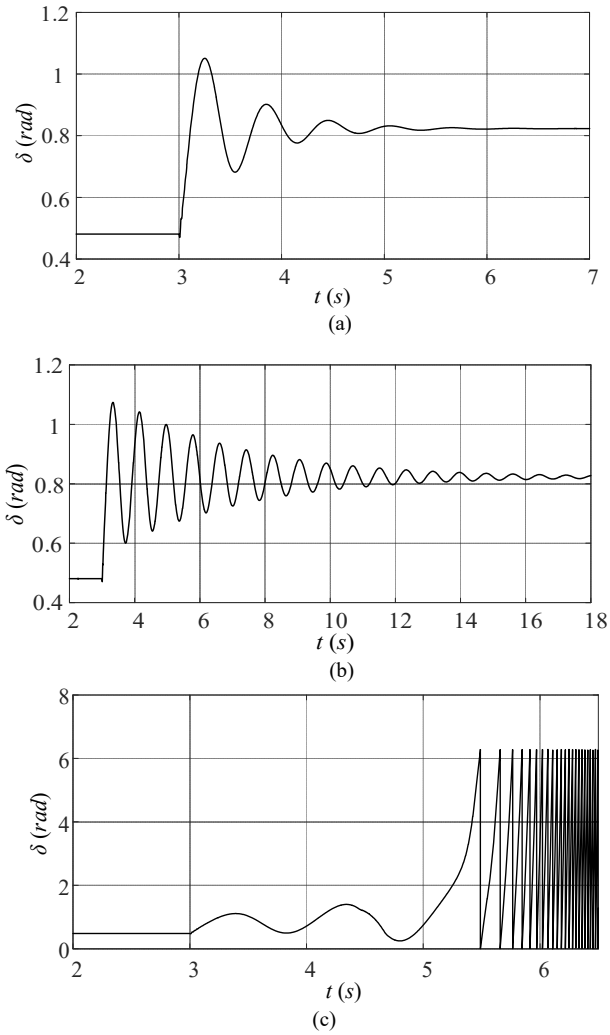

Fig. 4: Simulation results of the power angle with the decrease of k_{pdc} (a) $k_{pdc}=0.0080$ (b) $k_{pdc}=0.0040$ (c) $k_{pdc}=0.0024$.

when k_{pdc} keeps decreasing. It can be seen from the Fig. 4(a)-(c) that with the decrease of k_{pdc}, the power angles of GFM converter gradually deteriorate until lose synchronism with the grid. Therefore, the decrease of k_{pdc} is harmful to the transient stability of the system, which is consistent with the aforementioned analysis.

III. Internal Mechanism of the Parametric Effects of DVC

The qualitative influence law of the DVC parameters k_{pdc} on the transient stability of the system has been analyzed above, but the internal mechanism behind the influence law has not been revealed yet. At present, the equivalent damping method [5] and equal area criterion [9] mentioned in the published literature are often used in first-order or second-order systems to reveal internal mechanism. However, they cannot be applied to the GFM converter in this study which is actually a three-order system. In view of this, the bifurcation theory which has no restrictions on the order of applicable objects, is adopted to reveal the internal mechanism behind the influence of DVC parameters. The detailed analysis is as follows.

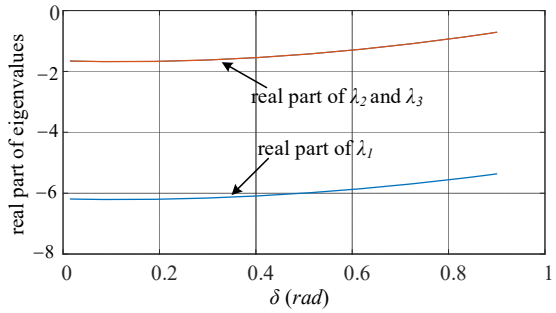

Fig. 5: The real part of the Jacobian matrix eigenvalues of equation (1).

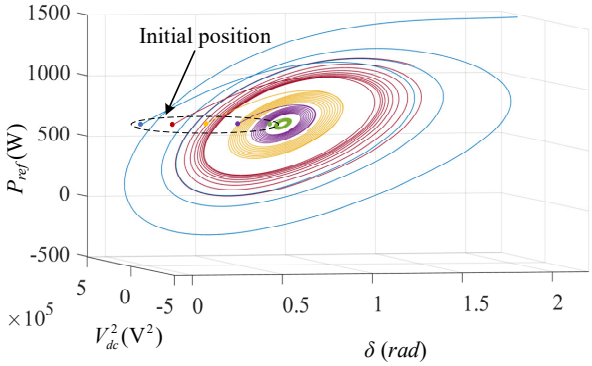

Fig. 6: Manifolds starting from different initial points when k_{pdc}=0.00360, k_{idc}=0.0250.

A. Internal mechanism of the influence of k_{pdc}

The real part of the eigenvalues of the Jacobian matrix of the differential equations (1) could be obtained as shown in Fig. 5. According to Fig. 5, the eigenvalues of Jacobian matrix will be affected by the power angle δ. Nevertheless, the Jacobian matrix typically have three eigenvalues, a negative real eigenvalue and a pair of conjugate complex eigenvalues with negative real parts. The absolute value of the negative real eigenvalue is much larger than the absolute value of the real part of the conjugate complex eigenvalues. Hence, the manifolds of the system quickly converge to the surface formed by the eigenvectors corresponding to λ_2 and λ_3 along the direction of the eigenvector corresponding to λ_1, and then gradually converge to the equilibrium point or gradually diverge [14]. In Fig. 6, it is shown a group of manifolds starting from different initial points with same k_{pdc}. These manifolds always first quickly converge to a surface and then gradually converge to the equilibrium point or gradually diverge, which is consistent with the previous analysis.

There is a limit cycle in the phase space, the following is the process of proving the existence of limit cycle. When the Poincaré section is selected as plane $(V_{dc})^2=(V_{dc}^{ref})^2$, the points of the Poincaré section can be obtained in two cases as shown in Fig. 7. Red points in Fig. 7 represent the converging process and blue points represent the diverging process. The only difference between the two cases is the initial position. Between these two cases, that is, at area A on the Poincaré section, there must be a phase trajectory that can return to itself. Therefore, there exists an unstable limit cycle at area A.

The ODE function in Matlab could be adopted to depict the positions of unstable limit cycles under different k_{pdc}, as shown in Fig. 8. When k_{pdc} gradually increases, the size of the

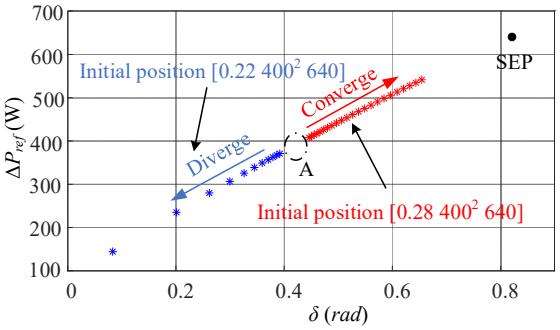

Fig. 7: Points on Poincaré section with the same k_{pdc} (k_{pdc}=0.0036).

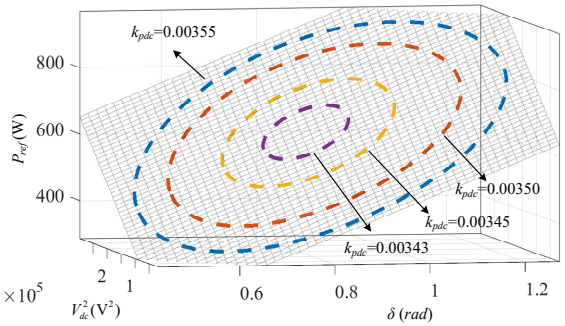

Fig. 8: Limit cycles in phase space with different k_{pdc}.

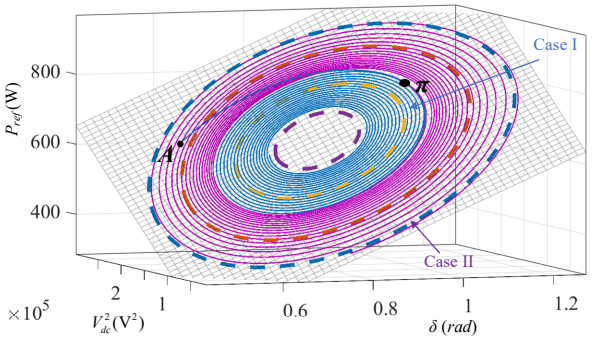

Fig. 9: Phase trajectories from same initial position under different k_{pdc} (initial position A: [0.517,400^2,640]; Case I (blue)：k_{pdc}=0.00355, Case II (purple)：k_{pdc}=0.00343)

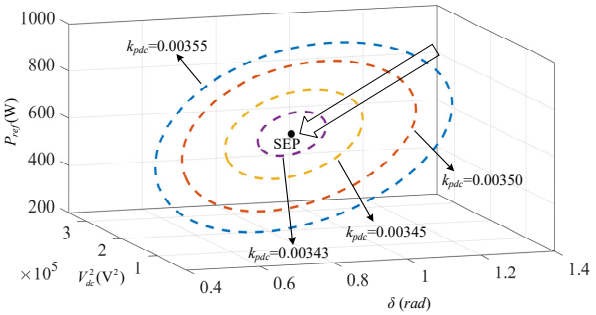

Fig. 10: Critical case of limit cycle with the decrease of k_{pdc}.

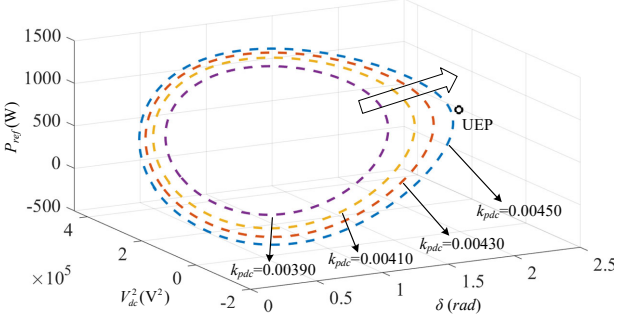

Fig. 11: Critical case of limit cycle with the increase of k_{pdc}.

unstable limit cycle continues to increase. These limit cycles are tangent to the non-principal subspace of the equilibrium point. There is little difference for the position of the non-principal subspace when k_{pdc} change slightly. Hence, the limit cycles under different k_{pdc} are approximately on a curved surface, as shown in Fig. 8.

When trajectories start from the same initial position under different k_{pdc}, due to the inconsistency of the size of the corresponding limit cycles, even if the intersection points of the phase trajectory and the curved surface are close, it may lead to different final states. As shown in Fig. 9, blue and purple trajectories represent two cases starting from the same initial position under different k_{pdc}. Their intersection points with the curved surface are very close, as shown in area π. The limit cycle corresponding to the k_{pdc} of blue trajectory is the smallest limit cycle, and the limit cycle corresponding to the k_{pdc} of purple trajectory is the largest limit cycle. The intersection points position (area π) is outside the blue limit cycle but inside the purple limit cycle. Therefore, the blue trajectory eventually diverges to infinity and the purple trajectory finally converges to stable equilibrium point. These two cases reveal that the essence of the influence of k_{pdc} on transient stability is that a small change in k_{pdc} will cause a drastic change in the size of the limit cycle, so that the phase trajectories that are close initially will reach different final states. A large k_{pdc} will lead to a large limit cycle, which allows more phase trajectories to converge to the stable equilibrium point, thereby ensuring better transient stability.

B. *Critical situations of limit cycles*

From the analysis above, it is known that the size of the limit cycle will gradually improve with the increase of k_{pdc}, which is beneficial to the transient stability. However, there are two critical situations for the change of limit cycles.

(a) The size of the limit cycle reduces with the decrease of k_{pdc} until it touches the equilibrium point, as shown in Fig. 10. After that, the system will undergo subcritical Hopf bifurcation and the equilibrium point will become unstable. Under this circumstance, phase trajectories from any initial points will diverge to infinity [15];

(b) The size of the limit cycle improves with the increase of k_{pdc}, as shown in Fig. 11. When the unstable limit cycle touches the unstable equilibrium point (saddle focus) of the system or the main subspace corresponding to the saddle focus, the system will undergo Homoclinic bifurcation [15]. Under this circumstance, the limit cycle will disappear and the stable manifolds of the unstable equilibrium point will become the boundary of the region of attraction (ROA).

In summary, with the increase of k_{pdc}, the dynamic characteristic of the GFM converter and the changes in the

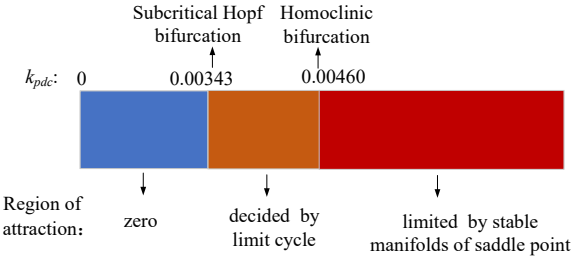

Fig. 12: Change of the system dynamics and the region of attraction as the of k_{pdc}.

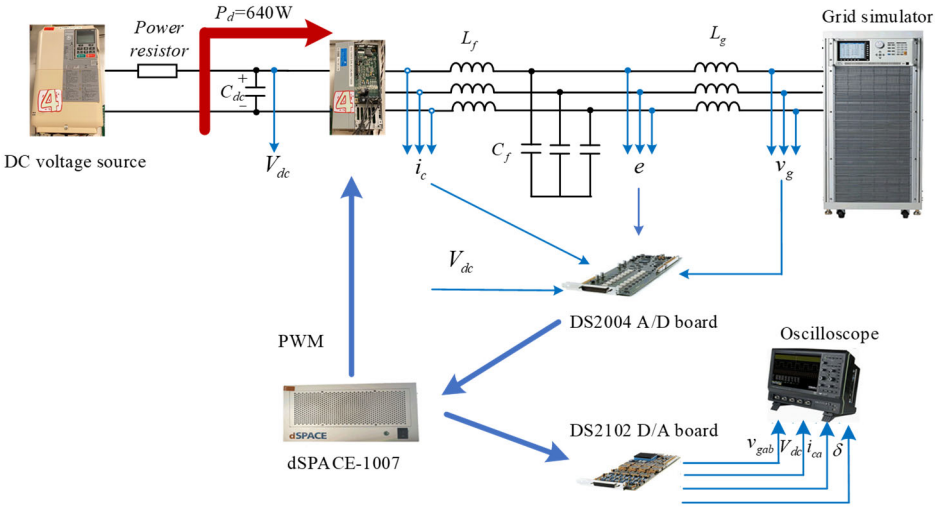

Fig. 13: Configuration of the experimental setup.

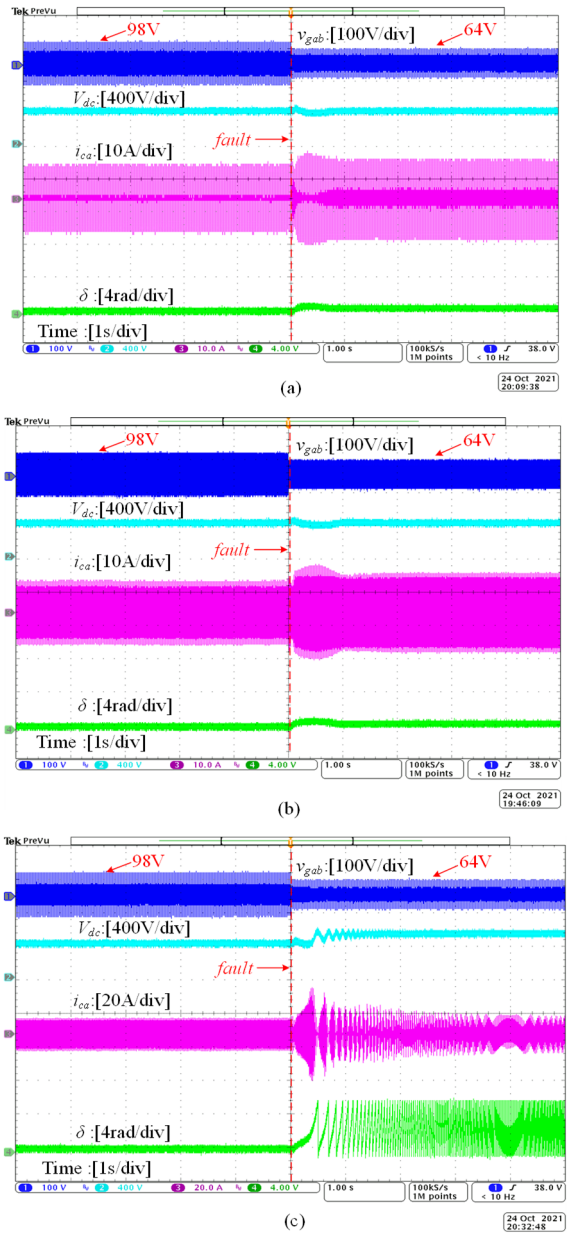

Fig. 14: When the grid voltage V_g drops from 1.0 p.u. to 0.65 p.u., the experimental dynamic responses of GFM converters (a) k_{pdc}=0.0080. (b) k_{pdc}=0.0040. (c) k_{pdc}=0.0024.

region of attraction are shown in Fig. 12. The limit cycle is first generated from subcritical Hopf bifurcation, and then disappears because of Homoclinic bifurcation. The boundary of the region of attraction is determined by the limit cycle before the Homoclinic bifurcation or by the stable manifolds of the saddle focus after Homoclinic bifurcation, respectively. Before Homoclinic bifurcation, with the increase of k_{pdc}, the limit cycle continuously enlarges, which could permit more initial points to converge to stable equilibrium point leading to a larger ROA.

Therefore, in order to ensure better transient stability of GFM converters, the value of k_{pdc} should be chosen as large as possible, which is consistent with the results of the phase portraits in section II.

IV. Experimental Results

In order to verify the effectiveness of the theoretical analysis, the experimental tests are conducted, where the main parameters listed in Table I are used for the setup. The photograph of the experimental setup is shown in Fig. 13, where the Chroma Grid Simulator 61845 is used to simulate the power grid. A DC voltage source connected with a power resistor is used to simulated the power source to inject constant power into the DC side of the GFM converter before and after fault. The PCC voltage $\boldsymbol{e}$, converter-side current $\boldsymbol{i_c}$, DC-Link voltage V_{dc} and grid voltage $\boldsymbol{v_g}$ are measured through the dSPACE DS2004 A/D board. The measured signals are sent to the dSPACE DS1007 platform to implement the DC-Link voltage control. The phase angles of $\boldsymbol{e}$ and $\boldsymbol{v_g}$ are measured by a fast PLL, and their phase difference, which is denoted as the power angle δ, is fed to the oscilloscope through the dSPACE DS2102 D/A board

Fig. 14 shows the experimental dynamic responses of the GFM converter with the decrease of k_{pdc} when the three-phase grid voltage drops from 1.0 p.u. to 0.65 p.u. From Fig. 14 (a)-(c), it is seen that, although the equilibrium point exists after fault, the GFM converter will lose synchronism with the grid when the k_{pdc} is small. The above observations are consistent with the theoretical analysis in section III.

V. Conclusions

In this paper, the phase portrait-based transient stability analysis reveals that the increase of k_{pdc} can enhance the transient stability of GFM converters. The internal mechanism of such parametric effect is that the subcritical Hopf bifurcation and the Homoclinic bifurcation will occur as the increase of k_{pdc}. The former give rise to the limit cycle and the latter make the limit cycle disappear. The boundary of ROA is the limit cycle before Homoclinic bifurcation. With the increase of k_{pdc}, the unstable limit cycle will expand. Then more initial points will be allowed to converge to equilibrium point leading to a larger ROA. Hence, the increase of k_{pdc} will enhance the transient stability of GFM converters. It is recommend selecting a large k_{pdc} when designing the DVC parameters. The experimental tests have verified the effectiveness of the theorical analysis.

REFERENCES

[1] F. Blaabjerg, R. Teodorescu, M. Liserre and A. V. Timbus, "Overview of Control and Grid Synchronization for Distributed Power Generation Systems," *IEEE Trans. Ind. Electron.*, vol. 53, no. 5, pp. 1398-1409, Oct. 2006.

[2] X. Wang, M. G. Taul, H. Wu, Y. Liao, F. Blaabjerg, and L. Harnefors, "Grid-synchronization stability of converter-based resources—An overview," *IEEE Open J. Ind. Appl.*, vol. 1, pp. 115–134, Aug. 2020.

[3] P. Kundur, *Power System Stability and Control*. New York, NY, USA: McGraw-Hill, 1994.

[4] H. Wu and X. Wang, "Design-Oriented Transient Stability Analysis of Grid-Connected Converters with Power Synchronization Control," *IEEE Trans. Ind. Electron.*, vol. 66, no. 8, pp. 6473-6482, Aug. 2019.

[5] D. Pan, X. Wang, F. Liu, and R. Shi, "Transient Stability of Voltage-Source Converters with Grid-Forming Control: A Design-Oriented Study," *IEEE J. Emerg. Select. Topics Power Electron.*, vol. 8, no. 2, pp. 1019-1033, Jun. 2020.

[6] X. Fu et al., "Large-Signal Stability of Grid-Forming and Grid-Following Controls in Voltage Source Converter: A Comparative Study," *IEEE Trans. on Power Electron.*, vol. 36, no. 7, pp. 7832-7840, Jul. 2021.

[7] J. Yang, C. K. Tse, M. Huang and X. Fu, "Homoclinic Bifurcation of a Grid-Forming Voltage Source Converter," *IEEE Trans. on Power Electron.*, vol. 36, no. 11, pp. 13176-13187, Nov. 2021.

[8] J. Guo et al., "Impedance Analysis and Stabilization of Virtual Synchronous Generators with Different DC-Link Voltage Controllers Under Weak Grid," *IEEE Trans. Ind. Electron.*, vol. 36, no. 10, pp. 11397-11408, Oct. 2021.

[9] H. Wu and X. Wang, "A Mode-Adaptive Power-Angle Control Method for Transient Stability Enhancement of Virtual Synchronous Generators," *IEEE J. Emerg. Select. Topics Power Electron.*, vol. 8, no. 2, pp. 1034-1049, Jun. 2020.

[10] W. Zhang, A. M. Cantarellas, J. Rocabert, A. Luna, and P. Rodriguez, "Synchronous Power Controller with Flexible Droop Characteristics for Renewable Power Generation Systems," *IEEE Trans. Sustain. Energy*, vol. 7, no. 4, pp. 1572–1582, May, 2016.

[11] P. Hart and B. Lesieutre, "Energy function for a grid-tied, droop controlled inverter," *in Proc. North Amer. Power Symp. (NAPS)*, Pullman, WA, USA, Sep. 2014.

[12] H. Yuan, X. Yuan and J. Hu, "Modeling of Grid-Connected VSCs for Power System Small-Signal Stability Analysis in DC-Link Voltage Control Timescale," *IEEE Trans. Power Syst.*, vol. 32, no. 5, pp. 3981-3991, Sep. 2017.

[13] S. H. Strogatz, *Nonlinear Dynamics and Chaos: With Applications to Physics, Biology, Chemistry, and Engineering*. New York, NY, USA: Perseus Books, 1994.

[14] Yuri A.Kuznetsov, *Elements of Applied Bifurcation Theory*, New York, NY, USA: Springer-Verlag, 2004.

[15] Steven H.Strogatz, *Nonlinear Dynamics and Chaos with Student Solutions Manual-with Applications to Physics, Biology, Chemistry and Engineering*, Second Edition, Florida, FL,CRC Press, 2014.